Innovative Systems Design and Engineering
ISSN 2222-1727 (Paper) ISSN 2222-2871 (Online)
Vol 3, No 6, 2012


# Simulation of Generation Process for Asymmetric Involute Gear Tooth Shape with and without Profile Correction

Mohammad Qasim Abdullah*
Department of Mechanical Engineering, College of Engineering, University of Baghdad, Baghdad, Iraq
*E-mail of the corresponding author: mohq1969@yahoo.com
Muhsin Jabir Jweeg
Department of Mechanical Engineering, College of Engineering, Al-Nahrain University, Baghdad, Iraq
E-mail: muhsinjj@yahoo.com

**Abstract**

In order to achieve any design study on a gear tooth or to carry out any type of analysis on a complete gear drive, the first step is the representation of the actual form of this tooth under consideration. In this work, a mathematical simulation of generation process for the symmetric involute gear teeth shapes based on the principle of the gear shaping process with a rack-shaped cutter has been developed to take into account the effect of asymmetric tooth profiles and the use of profile correction on each side of tooth with different design parameters for each side of tooth. As a result of this work, a computer program based on this mathematical simulation has been built to represent graphically step-by-step the actual form of symmetric and asymmetric gear teeth shapes with and without profile correction for different gear design parameters.

**Keywords:** Involute Gear Teeth, Symmetric, Asymmetric, Profile Correction, Mathematical Simulation, Generation Process.

## 1. Introduction

In this work, the principle of gear shaping process with a rack-shaped cutter which is one of the gear generation methods [1], has been adopted to simulate mathematically the generation process of involute gear teeth shapes. By this process the tooth profile obtained is composed of two well defined parts, the involute part and root fillet part. The involute part is generated by the straight sides of the rack cutter, whereas the root fillet part is formed by the cutter nose. In this mathematical simulation, two cases have been considered, the first case is for the generation of symmetric tooth shape and the second case has been developed to generate asymmetric involute gear teeth shapes with and without profile correction (profile shift) for different design parameters of module and number of teeth on gear, as well as pressure angles, root fillet radii, top edged radii and correction factors for loaded and unloaded tooth sides.

## 2. Generation of Symmetric Tooth

In the generation process of symmetric tooth shape, the generating rack cutter and gear blank roll in contact in timed relation to each other simultaneously, they are also given a feed relative to each other to remove the metal from the blank. In this process, the cutting tool (rack cutter) which shown in (Figure 1) is given a shape conjugate with the form of the tooth to be cut. Therefore; the geometrical representation of the rack cutter with its rolling simulation are imperative.

### *2.1 Geometrical Representation of Rack Cutter*

The basic rack cutter which is shown in (Figure 1) has been adopted as a cutting tool for this generation process [2]. Fifteen points are used to define the outer shape of this rack cutter. The Cartesian coordinates of these points are measured with respect to a reference point $P(0,0)$ which is located on the pitch line $TT$.

Referring to (Figure 1), it can be that:

from $\triangle C_1CD$: $C_1D = \frac{r_{fu}}{\cos\phi}$ (1)

 

also, from $\triangle\ Q_1S_1D$: $S_1D = r_{fu}\ tan\ \phi$ (2)

and $Q_1D = \frac{r_{fu}}{cos\ \phi}$ (3)

now, $Q_1B = C_1S_1 = C_1D - S_1D$ (4)

By substituting equation (1) and equation (2) into equation (4), yields:

$$Q_1B = \frac{r_{fu}}{cos\ \phi}\ (1 - sin\ \phi) \quad (5)$$

Therefore; $H_1 = -\left[\frac{p_c}{4} + h_d\ tan\ \phi + \frac{r_{fu}}{cos\ \phi}\ (1 - sin\ \phi)\right]$ (6)

$$K_1 = -\ h_d + r_{fu} \quad (7)$$

In the same way, it can be proved that:

$$H_4 = \frac{p_c}{4} + h_d\ tan\ \phi + \frac{r_{fl}}{cos\ \phi}\ (1 - sin\ \phi) \quad (8)$$

$$K_4 = -\ h_d + r_{fl} \quad (9)$$

$$Q_4L = \frac{r_{fl}}{cos\ \phi} \quad (10)$$

and $Q_4N = \frac{r_{fl}}{cos\ \phi}\ (1 - sin\ \phi)$ (11)

Also, from the same figure, it can be shown that:

from $\triangle\ C_3JK$: $C_3K = \frac{r_{tl}}{cos\ \phi}$ (12)

also, from $\triangle\ Q_3S_3K$: $S_3K = r_{tl}\ tan\ \phi$ (13)

and $Q_3K = \frac{r_{tl}}{cos\ \phi}$ (14)

now, $Q_3I = C_3S_3 = C_3K - S_3K$ (15)

 

By substituting equation (12) and equation (13) into equation (15), yields:

$$Q_3I = \frac{r_{tl}}{\cos\phi}\ (1 - \sin\phi) \tag{16}$$

Therefore; $H_3 = \frac{p_c}{4} - h_a \tan\phi - \frac{r_{tl}}{\cos\phi}\ (1 - \sin\phi)$ (17)

$$K_3 = h_a - r_{tl} \tag{18}$$

In the same way, it can be proved that:

$$H_2 = -\left[\frac{p_c}{4} - h_a \tan\phi - \frac{r_{tu}}{\cos\phi}\ (1 - \sin\phi)\right] \tag{19}$$

$$K_2 = h_a - r_{tu} \tag{20}$$

$$Q_2E = \frac{r_{tu}}{\cos\phi} \tag{21}$$

and $Q_2G = \frac{r_{tu}}{\cos\phi}\ (1 - \sin\phi)$ (22)

Now, by referring to (Figure 1) again, the Cartesian coordinates of the geometrical points for the rack cutter can be found as shown below:

$$X_A = -\frac{p_c}{2}\ , \quad Y_A = -h_d$$

$$X_B = H_1\ , \quad Y_B = -h_d$$

$$AB = |X_B - X_A|\ , \quad CD = r_{fu} \tan\phi$$

$$X_D = H_1 + \frac{r_{fu}}{\cos\phi}\ , \quad Y_D = K_1$$

$$X_C = X_D - CD \sin\phi\ , \quad Y_C = Y_D - CD \cos\phi$$

$$X_E = H_2 - \frac{r_{tu}}{\cos\phi}\ , \quad Y_E = K_2$$

$$ED = \sqrt{(X_E - X_D)^2 + (Y_E - Y_D)^2}\ , \quad EF = r_{tu} \tan\phi$$

 

$$X_F = X_E + EF\ sin\ \phi \quad , \quad Y_F = Y_E + EF\ cos\ \phi$$

$$X_G = H_2 \quad , \quad Y_G = h_a$$

$$X_H = 0 \quad , \quad Y_H = h_a \quad , \quad GH = |X_H - X_G|$$

$$X_I = H_3 \quad , \quad Y_I = h_a$$

$$HI = |X_I - X_H| \quad , \quad KJ = r_{tl}\ tan\ \phi$$

$$X_K = H_3 + \frac{r_{tl}}{cos\ \phi} \quad , \quad Y_K = K_3$$

$$X_J = X_K - KJ\ sin\ \phi \quad , \quad Y_J = Y_K + KJ\ cos\ \phi$$

$$X_L = H_4 - \frac{r_{fl}}{cos\ \phi} \quad , \quad Y_L = K_4$$

$$KL = \sqrt{(X_L - X_K)^2 + (Y_L - Y_K)^2} \quad , \quad LM = r_{fl}\ tan\ \phi$$

$$X_M = X_L + LM\ sin\ \phi \quad , \quad Y_M = Y_L - LM\ cos\ \phi$$

$$X_N = H_4 \quad , \quad Y_N = -h_d$$

$$X_O = \frac{p_c}{2} \quad , \quad Y_O = -h_d \quad \text{and} \quad NO = |X_O - X_N|$$

Where $\phi$: is the pressure angle of symmetric tooth, it's the same for loaded and unloaded tooth sides,
$r_{fl}$ & $r_{tl}$: are the root fillet and top edged radii of loaded tooth side,
$r_{fu}$ & $r_{tu}$: are the root fillet and top edged radii of unloaded tooth side,
$h_a$ & $h_d$: are the addendum and dedendum heights of tooth,
$p_c$: is the circular pitch, $p_c = \pi\, m_o$ and $m_o$: is the module.

*2.2 Rolling Simulation of Rack Cutter*

For the tooth profiles generation, the essential requirement is that the pitch line TT which is shown in (Figure 1) rolls on the pitch circle of blank without slipping. In (Figure 2), the pitch circle with a center $O_1$ has been kept stationary while the pitch line TT rolls on it on either side of pitch point P. Also, in order to achieve the tooth profile correction, the pitch line TT must be withdrawn from the pitch circle by amount "$x.m_o$" where $x$ represents the correction factor [3]. According to this profile correction, new addendum and dedendum heights will be obtained, therefore:

$$h_a)_{new\ (after\ rolling)} = h_a)_{old\ (before\ rolling)} + x.m_o \qquad (23)$$

 

$$h_d)_{new\ (after\ rolling)} = h_d)_{old\ (before\ rolling)} - x.m_o \quad (24)$$

The generation process is carried out by the rolling of a whole rack cutter to the right and left directions from the initial position without slipping by incremental angles ($\theta$'s) until a whole tooth shape is generated, then from (Figure 2), it can be shown that:

Firstly, according to the principle of involute construction, [4]:

$$L_1 = R_p.\theta \quad (25)$$

and $$inv\,\phi = \tan\phi - \phi \quad (26)$$

Also, from the same figure, $$L_2 = \sqrt{{R_p}^2 + {L_1}^2} \quad (27)$$

and $$L_3 = \sqrt{{L_2}^2 + {R_p}^2 - 2\,R_p\,L_2\cos(inv\,\phi)} \quad (28)$$

where $R_p$: represents the radius of pitch circle, $R_p = \frac{m_o.z}{2}$ and $z$: represents the number of teeth on a gear.

Therefore; the rolling simulation of a rack cutter can be achieved in the following procedure.

2.2.1 Rolling Simulation of A Whole Rack Cutter to Right Direction

Referring to Fig.(3.5), it can be found the Cartesian coordinates of rack points for the right direction ($A', B', C', D', E', F', G', H', I', J', K', L', M', N', and\ O'$) are as follows:

$$X_{H'} = (L_3 + h_a).sin\,\theta \quad , \quad Y_{H'} = (L_3 + h_a).cos\,\theta$$

$$X_{G'} = X_{H'} - GH.\cos\theta \quad , \quad Y_{G'} = Y_{H'} + GH.sin\,\theta$$

$$X_{Q_2'} = X_{H'} - (GH + GQ_2).cos\,\theta \quad , \quad Y_{Q_2'} = Y_{H'} + (GH + GQ_2).sin\,\theta$$

$$X_{E'} = X_{Q_2'} - Q_2E.sin(\theta + \phi) \quad , \quad Y_{E'} = Y_{Q_2'} - Q_2E.cos(\theta + \phi)$$

$$X_{F'} = X_{Q_2'} - (Q_2E - EF).sin(\theta + \phi) \quad , \quad Y_{F'} = Y_{Q_2'} - (Q_2E - EF).cos(\theta + \phi)$$

$$H_2' = X_{G'} - r_{tu}.sin\,\theta \quad , \quad K_2' = Y_{G'} - r_{tu}.cos\,\theta$$

$$X_{D'} = X_{Q_2'} - (Q_2E + ED).sin(\theta + \phi) \quad , \quad Y_{D'} = Y_{Q_2'} - (Q_2E + ED).cos(\theta + \phi)$$

$$X_{C'} = X_{Q_2'} - (Q_2E + ED + DC).sin(\theta + \phi) \quad , \quad Y_{C'} = Y_{Q_2'} - (Q_2E + ED + DC).cos(\theta + \phi)$$

 

$$X_{Q_1'} = X_{Q_2'} - (Q_2E + ED + DQ_1).sin(\theta + \phi) \quad , \quad Y_{Q_1'} = Y_{Q_2'} - (Q_2E + ED + DQ_1).cos(\theta + \phi)$$

$$X_{B'} = X_{Q_1'} - Q_1B.\cos\theta \quad , \quad Y_{B'} = Y_{Q_1'} + Q_1B.sin\,\theta$$

$$X_{A'} = X_{Q_1'} - (Q_1B + AB).\cos\theta \quad , \quad Y_{A'} = Y_{Q_1'} + (Q_1B + AB).sin\,\theta$$

$$H_1' = X_{B'} + r_{fu}.sin\,\theta \quad , \quad K_1' = Y_{B'} + r_{fu}.cos\,\theta$$

$$X_{I'} = X_{H'} + HI.\cos\theta \quad , \quad Y_{I'} = Y_{H'} - HI.sin\,\theta$$

$$X_{Q_2'} = X_{H'} + (HI + IQ_3).cos\,\theta \quad , \quad Y_{Q_2'} = Y_{H'} - (HI + IQ_3).sin\,\theta$$

$$X_{K'} = X_{Q_2'} - Q_3K.sin(\theta - \phi) \quad , \quad Y_{K'} = Y_{Q_2'} - Q_3K.cos(\theta - \phi)$$

$$X_{J'} = X_{Q_2'} + (Q_3K - KJ).sin(\theta - \phi) \quad , \quad Y_{J'} = Y_{Q_2'} - (Q_3K - KJ).cos(\theta - \phi)$$

$$H_3' = X_{I'} - r_{tl}\,sin\,\theta \quad , \quad K_3' = Y_{I'} - r_{tl}\,cos\,\theta$$

$$X_{L'} = X_{Q_2'} - (Q_2K + KL).sin(\theta - \phi) \quad , \quad Y_{L'} = Y_{Q_2'} - (Q_2K + KL).cos(\theta - \phi)$$

$$X_{C'} = X_{Q_2'} - (Q_2K + KL + LM).sin(\theta - \phi) \quad , \quad Y_{C'} = Y_{Q_2'} - (Q_2K + KL + LM).cos(\theta - \phi)$$

$$X_{Q_4'} = X_{Q_2'} - (Q_2K + KL + LQ_4).sin(\theta - \phi) \quad , \quad Y_{Q_4'} = Y_{Q_2'} - (Q_2K + KL + LQ_4).cos(\theta - \phi)$$

$$X_{N'} = X_{Q_4'} + Q_4N.\cos\theta \quad , \quad Y_{N'} = Y_{Q_4'} - Q_4N.sin\,\theta$$

$$X_{O'} = X_{Q_4'} + (Q_4N + NO).\cos\theta \quad , \quad Y_{O'} = Y_{Q_4'} - (Q_4N + NO).sin\,\theta$$

$$H_4' = X_{N'} + r_{fl}.sin\,\theta \quad ,$$

$$K_4' = Y_{N'} + r_{fl}.cos\,\theta$$

*2*.2.2 Rolling Simulation of A Whole Rack Cutter to Left Direction

In order to find the coordinates of rack points for the left direction ($A''$, $B''$, $C''$, $D''$, $E''$, $F''$, $G''$, $H''$, $I''$, $J''$, $K''$, $L''$, $M''$, $N''$, *and* $O''$), the same previous procedure of rolling simulation for the right direction can be done but with replacing the angle $(\theta)$ by $(-\theta)$.

**3. Generation of Asymmetric Tooth**

In this case, there are different profiles on each side of tooth, therefore; there are two different pressure angles for both sides of tooth, the first is for loaded side "$\phi_l$" and the other is for unloaded side "$\phi_u$". In this case, the generation process for the symmetric tooth must be developed to take into account this asymmetry of the tooth profiles. Therefore; the generation process of tooth must be carried out into two stages, the first for loaded side part

 

and the other for unloaded side part.

*3.1 Generation Process for Loaded Side Part of Tooth*

By this stage, the rolling simulation of a half rack cutter (right half) to the right and left directions from the initial position without slipping by incremental angles ($\theta$'s) is carried out until a half tooth shape (loaded side part of the tooth) would be generated. Also, to achieve the tooth profile correction of this side, the pitch line $TT$ must be withdrawn from the pitch circle by amount "$x_l . m_o$" where $x_l$ represents the correction factor for loaded side of tooth as shown in (Figure 3). Therefore; the new addendum and dedendum heights for the loaded side of tooth are:

$$h_a)_{new\ (after\ rolling)} = h_a)_{old\ (before\ rolling)} + x_l . m_o \quad (29)$$

$$h_d)_{new\ (after\ rolling)} = h_d)_{old\ (before\ rolling)} - x_l . m_o \quad (30)$$

Now, from the principle of involute construction for unloaded side part of tooth, it can be shown that:

$$L_1 = R_p . \theta \quad (31)$$

$$inv\ \phi_l = \tan \phi_l - \phi_l \quad (32)$$

$$L_2 = \sqrt{{R_p}^2 + {L_1}^2} \quad (33)$$

and $$L_3 = \sqrt{{L_2}^2 + {R_p}^2 - 2\, R_p\, L_2 \cos(inv\ \phi_l)} \quad (34)$$

where $\phi_l$: represents the pressure angle of loaded side of tooth.

Then, the rolling simulation of the loaded side part of tooth can be achieved in the following procedure.

3.1.1 Rolling Simulation of Right Half Rack to Right Direction

Referring to (Figure 3), it can be found that:

$$X_{H'} = (L_3 + h_a) . sin\ \theta \quad , \quad Y_{H'} = (L_3 + h_a) . cos\ \theta$$

$$X_{I'} = X_{H'} + HI . \cos\theta \quad , \quad Y_{I'} = Y_{H'} - HI . sin\ \theta$$

$$X_{Q_3'} = X_{H'} + (HI + IQ_3) . cos\ \theta \quad , \quad Y_{Q_3'} = Y_{H'} - (HI + IQ_3) . sin\ \theta$$

$$X_{K'} = X_{Q_3'} - Q_3K . sin(\theta - \phi_l) \quad , \quad Y_{K'} = Y_{Q_3'} - Q_3K . cos(\theta - \phi_l)$$

$$X_{J'} = X_{Q_3'} + (Q_3K - KJ) . sin(\theta - \phi_l) \quad , \quad Y_{J'} = Y_{Q_3'} - (Q_3K - KJ) . cos(\theta - \phi_l)$$

$$H_3' = X_{I'} - r_{tl} \sin\theta \quad , \quad K_3' = Y_{I'} - r_{tl} \cos\theta$$

$$X_{L'} = X_{Q_2'} - (Q_2K + KL) . sin(\theta - \phi_l) \quad , \quad Y_{L'} = Y_{Q_2'} - (Q_2K + KL) . cos(\theta - \phi_l)$$

$$X_{M'} = X_{Q_2'} - (Q_2K + KL + LM) . sin(\theta - \phi_l) \quad , \quad Y_{M'} = Y_{Q_2'} - (Q_2K + KL + LM) . cos(\theta - \phi_l)$$

 

$$X_{Q_4}{}' = X_{Q_2}{}' - (Q_2K + KL + LQ_4).sin(\theta - \phi_l) \quad , \quad Y_{Q_4}{}' = Y_{Q_2}{}' - (Q_2K + KL + LQ_4).cos(\theta - \phi_l)$$

$$X_{N'} = X_{Q_4}{}' + Q_4N.\cos\theta \quad , \quad Y_{N'} = Y_{Q_4}{}' - Q_4N.\sin\theta$$

$$X_{O'} = X_{Q_4}{}' + (Q_4N + NO).\cos\theta \quad , \quad Y_{O'} = Y_{Q_4}{}' - (Q_4N + NO).\sin\theta$$

$$H_4' = X_{N'} + r_{fl}.\sin\theta \quad , \quad K_4' = Y_{N'} + r_{fl}.\cos\theta$$

3.1.2 Rolling Simulation of Right Half Rack to Left Direction

Also, by referring to (Figure 3), it can be found that:

$$X_{H''} = -(L_3 + h_a).\sin\theta \quad , \quad Y_{H''} = (L_3 + h_a).\cos\theta$$

$$X_{I''} = X_{H''} + HI.\cos\theta \quad , \quad Y_{I''} = Y_{H''} + HI.\sin\theta$$

$$X_{Q_2}{}'' = X_{H''} + (HI + IQ_3).cos\,\theta \quad , \quad Y_{Q_2}{}'' = Y_{H''} + (HI + IQ_3).sin\,\theta$$

$$X_{K''} = X_{Q_2}{}'' + Q_3K.sin(\theta + \phi_l) \quad , \quad Y_{K''} = Y_{Q_2}{}'' - Q_3K.cos(\theta + \phi_l)$$

$$X_{J''} = X_{Q_2}{}'' + (Q_3K - Kf).sin(\theta + \phi_l) \quad , \quad Y_{J''} = Y_{Q_2}{}'' - (Q_3K - Kf).cos(\theta + \phi_l)$$

$$H_3'' = X_{I''} + r_{tl}\,sin\theta \quad , \quad K_3'' = Y_{I''} - r_{tl}\,cos\,\theta$$

$$X_{L''} = X_{Q_2}{}'' + (Q_3K + KL).sin(\theta + \phi_l) \quad , \quad Y_{L''} = Y_{Q_2}{}'' - (Q_3K + KL).cos(\theta + \phi_l)$$

$$X_{M''} = X_{Q_2}{}'' + (Q_3K + KL + LM).sin(\theta + \phi_l) \quad , \quad Y_{M''} = Y_{Q_2}{}'' - (Q_3K + KL + LM).cos(\theta + \phi_l)$$

$$X_{Q_4}{}'' = X_{Q_2}{}'' + (Q_3K + KL + LQ_4).sin(\theta + \phi_l) \quad , \quad Y_{Q_4}{}'' = Y_{Q_2}{}'' - (Q_3K + KL + LQ_4).cos(\theta + \phi_l)$$

$$X_{N''} = X_{Q_4}{}'' + Q_4N.\cos\theta \quad , \quad Y_{N''} = Y_{Q_4}{}'' + Q_4N.\sin\theta$$

$$X_{O''} = X_{Q_4}{}'' + (Q_4N + NO).\cos\theta \quad , \quad Y_{O''} = Y_{Q_4}{}'' + (Q_4N + NO).\sin\theta$$

$$H_4'' = X_{N''} - r_{fl}.\sin\theta \quad , \quad K_4'' = Y_{N''} + r_{fl}.\cos\theta$$

*3.2 Generation Process for Unloaded Side Part of Tooth*

By this stage, the rolling simulations of the second half rack cutter (left half of rack cutter) to the right and left directions from the initial position without slipping by incremental angles ($\theta$'s) until the another half tooth shape (loaded side part of the tooth) is generated and to achieve the tooth addendum modification of this side, the pitch line $TT$ must be withdrawn from the pitch circle by amount "$x_u.m_o$" where $x_u$ represents the correction factor for unloaded side of tooth as shown in (Figure 4). Therefore; the new addendum and dedendum heights for unloaded side of tooth are:

 

$$h_a)_{new\ (after\ rolling)} = h_a)_{old\ (before\ rolling)} + x_u . m_o \quad (35)$$

$$h_d)_{new\ (after\ rolling)} = h_d)_{old\ (before\ rolling)} - x_u . m_o \quad (36)$$

Also, from the principle of involute construction of the unloaded side part of tooth, it can be shown that:

$$L_4 = R_p . \theta \quad (37)$$

$$inv\ \phi_u = \tan \phi_u - \phi_u \quad (38)$$

$$L_5 = \sqrt{{R_p}^2 + {L_4}^2} \quad (39)$$

and $$L_6 = \sqrt{{L_5}^2 + {R_p}^2 - 2\ R_p\ L_5 \cos(inv\ \phi_u)} \quad (40)$$

where $\phi_u$: represents the pressure angle of unloaded side of tooth.

Then, the rolling simulation of the unloaded side part of tooth can be achieved in the following procedure.

3.2.1 Rolling Simulation of Left Half Rack to Right Direction

Referring to (Figure 4), it can be found that:

$$X_{H'} = (L_6 + h_a) . sin\ \theta \quad , \quad Y_{H'} = (L_6 + h_a) . cos\ \theta$$

$$X_{G'} = X_{H'} - GH . \cos\theta \quad , \quad Y_{G'} = Y_{H'} + GH . sin\ \theta$$

$$X_{Q_2'} = X_{H'} - (GH + GQ_2) . cos\ \theta \quad , \quad Y_{Q_2'} = Y_{H'} + (GH + GQ_2) . sin\ \theta$$

$$X_{E'} = X_{Q_2'} - Q_2E . sin(\theta + \phi_u) \quad , \quad Y_{E'} = Y_{Q_2'} - Q_2E . cos(\theta + \phi_u)$$

$$X_{F'} = X_{Q_2'} - (Q_2E - EF) . sin(\theta + \phi_u) \quad , \quad Y_{F'} = Y_{Q_2'} - (Q_2E - EF) . cos(\theta + \phi_u)$$

$$H_2' = X_{G'} - r_{tu} . sin\ \theta \quad , \quad K_2' = Y_{G'} - r_{tu} . cos\ \theta$$

$$X_{D'} = X_{Q_2'} - (Q_2E + ED) . sin(\theta + \phi_u) \quad , \quad Y_{D'} = Y_{Q_2'} - (Q_2E + ED) . cos(\theta + \phi_u)$$

$$X_{C'} = X_{Q_2'} - (Q_2E + ED + DC) . sin(\theta + \phi_u) \quad , \quad Y_{C'} = Y_{Q_2'} - (Q_2E + ED + DC) . cos(\theta + \phi_u)$$

$$X_{Q_1'} = X_{Q_2'} - (Q_2E + ED + DQ_1) . sin(\theta + \phi_u) \quad , \quad Y_{Q_1'} = Y_{Q_2'} - (Q_2E + ED + DQ_1) . cos(\theta + \phi_u)$$

$$X_{B'} = X_{Q_1'} - Q_1B . \cos\theta \quad , \quad Y_{B'} = Y_{Q_1'} + Q_1B . sin\ \theta$$

 

$$X_{A'} = X_{Q_1'} - (Q_1B + AB).\cos\theta \quad , \quad Y_{A'} = Y_{Q_1'} + (Q_1B + AB).\sin\theta$$

$$H_1' = X_{B'} + r_{fu}.\sin\theta \quad , \quad K_1' = Y_{B'} + r_{fu}.\cos\theta$$

3.2.2 Rolling Simulation of Left Half Rack to Left Direction

Also, by referring to (Figure 4), it can be found that:

$$X_{H''} = -(L_6 + h_a).\sin\theta \quad , \quad Y_{H''} = (L_6 + h_a).\cos\theta$$

$$X_{G''} = X_{H''} - GH.\cos\theta \quad , \quad Y_{G''} = Y_{H''} - GH.\sin\theta$$

$$X_{Q_2''} = X_{H''} - (GH + GQ_2).\cos\theta \quad , \quad Y_{Q_2''} = Y_{H''} - (GH + GQ_2).\sin\theta$$

$$X_{E''} = X_{Q_2''} + Q_2E.\sin(\theta - \phi_u) \quad , \quad Y_{E''} = Y_{Q_2''} - Q_2E.\cos(\theta - \phi_u)$$

$$X_{F''} = X_{Q_2''} + (Q_2E - EF).\sin(\theta - \phi_u) \quad , \quad Y_{F''} = Y_{Q_2''} - (Q_2E - EF).\cos(\theta - \phi_u)$$

$$H_2'' = X_{G''} + r_{tu}.\sin\theta \quad , \quad K_2'' = Y_{G''} - r_{tu}.\cos\theta$$

$$X_{D''} = X_{Q_2''} + (Q_2E + ED).\sin(\theta - \phi_u) \quad , \quad Y_{D''} = Y_{Q_2''} - (Q_2E + ED).\cos(\theta - \phi_u)$$

$$X_{C''} = X_{Q_2''} + (Q_2E + ED + DC).\sin(\theta - \phi_u) \quad , \quad Y_{C''} = Y_{Q_2''} - (Q_2E + ED + DC).\cos(\theta - \phi_u)$$

$$X_{Q_1''} = X_{Q_2''} + (Q_2E + ED + DQ_1).\sin(\theta - \phi_u) \quad , \quad Y_{Q_1''} = Y_{Q_2''} - (Q_2E + ED + DQ_1).\cos(\theta - \phi_u)$$

$$X_{B''} = X_{Q_1''} - Q_1B.\cos\theta \quad , \quad Y_{B''} = Y_{Q_1''} - Q_1B.\sin\theta$$

$$X_{A''} = X_{Q_1''} - (Q_1B + AB).\cos\theta \quad , \quad Y_{A''} = Y_{Q_1''} - (Q_1B + AB).\sin\theta$$

$$H_1'' = X_{B''} - r_{fu}.\sin\theta \quad , \quad K_1'' = Y_{B''} + r_{fu}.\cos\theta$$

Finally, in order to represent the final shape of asymmetric tooth, the two generated parts of loaded and unloaded sides of tooth are joined together with taking into account the vertical shift difference between these two generated parts with amount $(L_6 - L_3)$, (i.e. the Y-coordinate of each point on the generated unloaded side must be shifted downward by this amount when $\phi_u > \phi_l$ and upward when $\phi_u < \phi_l$.

**4. Results**

A computer program based on the above mathematical simulation using has been built using Microsoft Quick-BASIC (ver. 4.5) to represent graphically the symmetric and asymmetric gear teeth shapes with and without profile correction for different gear design parameters of module and number of teeth on gear, addendum and dedendum heights as well as pressure angles, root fillet radii, top edged radii and correction factors for loaded and unloaded tooth sides. (Figure 5) and (Figure 6) shows selective samples for symmetric and asymmetric involute gear teeth shapes respectively, which are generated by this program.

 

## 5. Conclusions

In this work, a developed mathematical simulation of generation process for asymmetric involute gear teeth shapes with and without profile correction for different gear design parameters of loaded and unloaded tooth sides has been presented. Also, a computer program based on this mathematical simulation has been built to represent graphically step-by-step the actual form of these gear teeth shapes.

## References

[1] Marinov, V. (2006). *Manufacturing Technology*. (5th ed.). Pearson Education Inc., USA.

[2] Litvin, F. L. (1997). *Development of Gear Technology and Theory of Gearing*. NASA Reference Publication 1406, USA.

[3] Litvin, F. L., and Fuentes, A. (2004). *Gear Geometry and Applied Theory*. (2nd ed.). Cambridge University Press, New York, USA.

[4] Maitra, G. M. (1994). *Handbook of Gear Design*. (2nd ed.). Tata McGraw-Hill Publishing Company Limited, New Delhi.

 

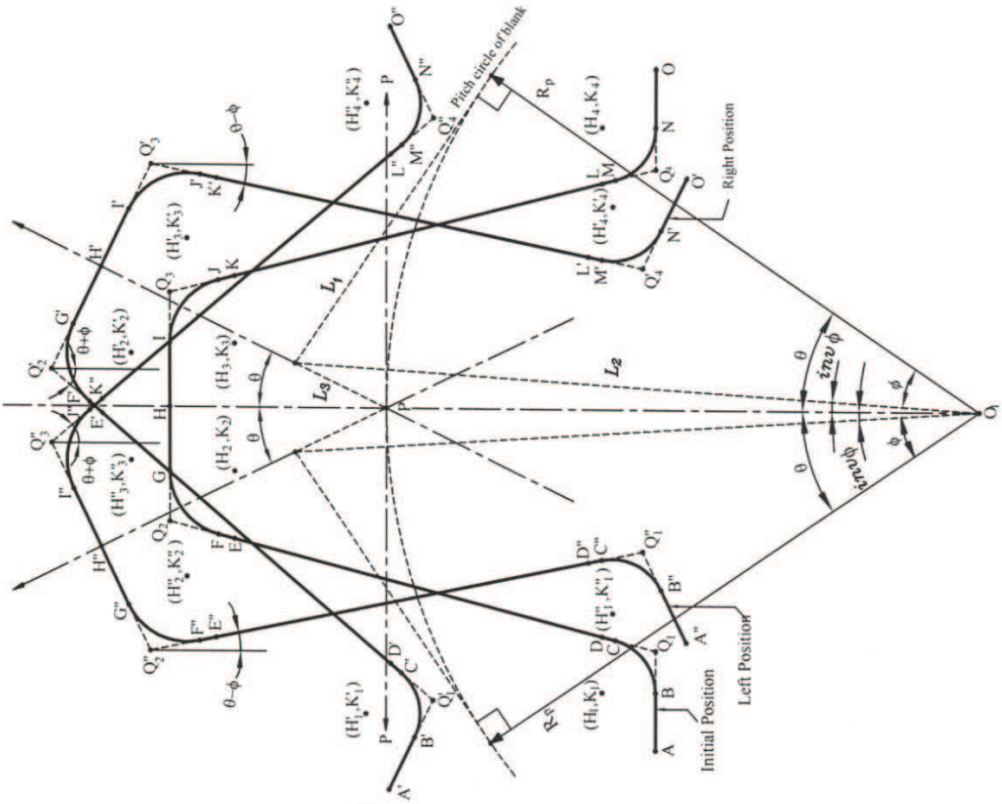


Figure 2. Rolling of a whole rack cutter.

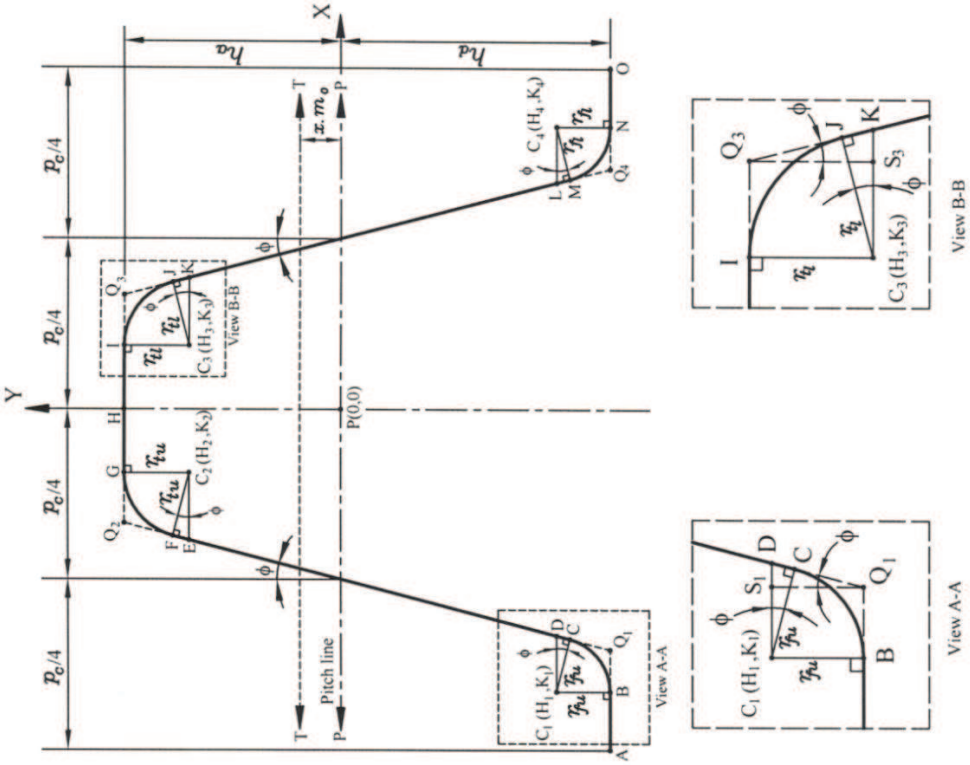


Figure 1. Basic rack cutter.

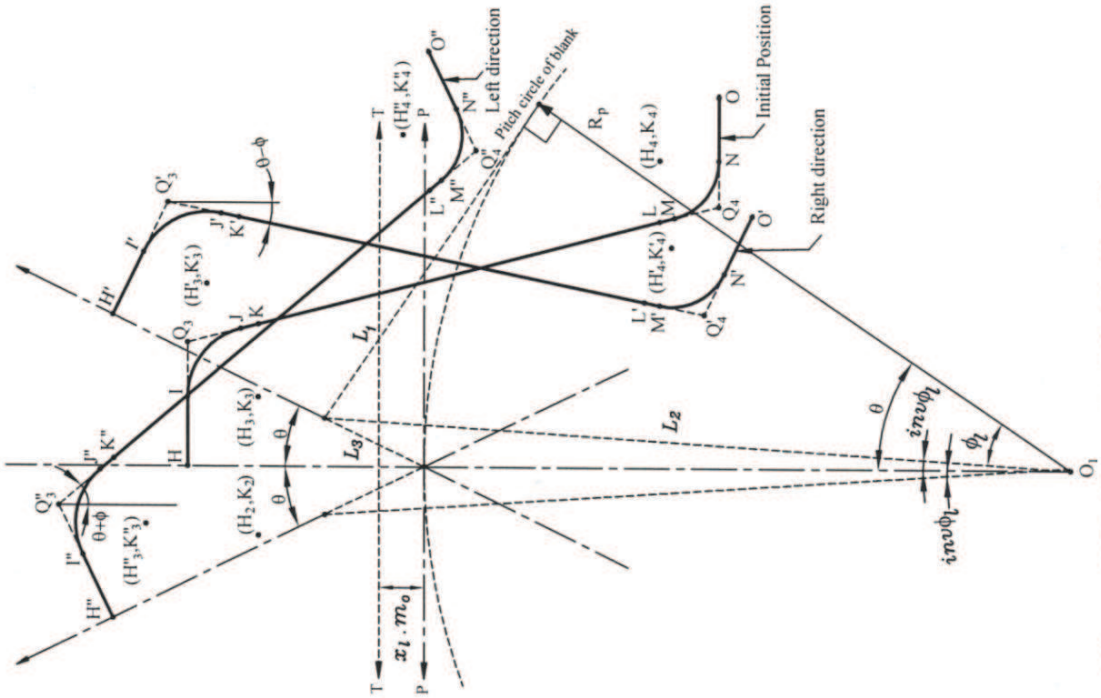


Figure 4. Rolling of a right half rack cutter to the right and left directions.

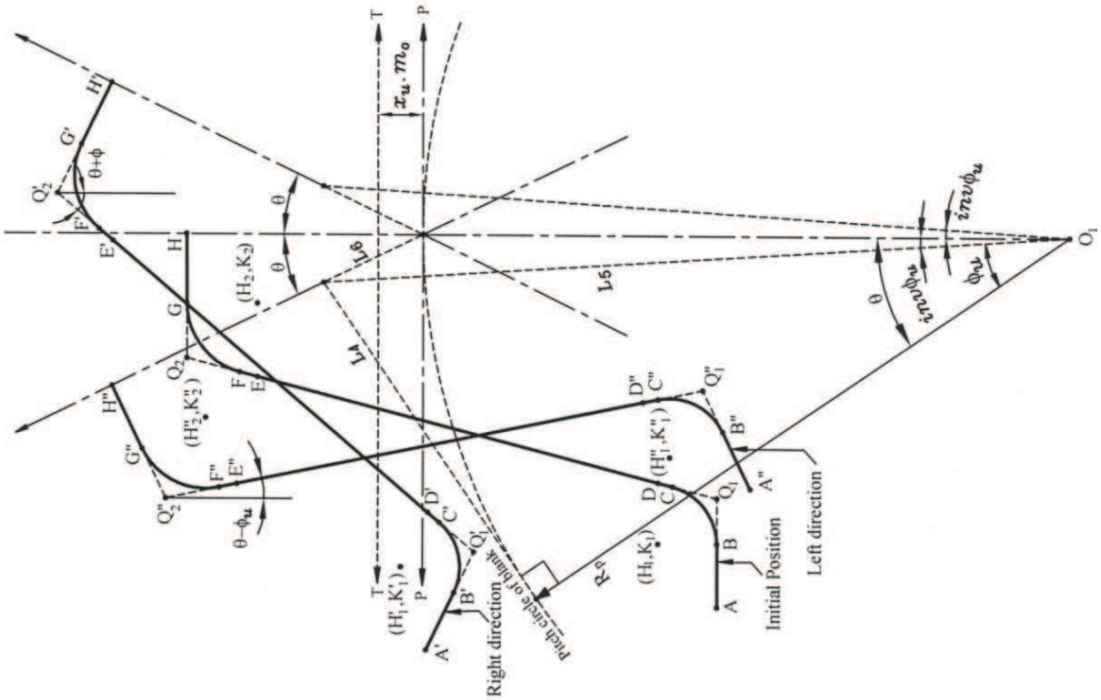

Figure 3. Rolling of a left half rack cutter to the right and left directions.

 

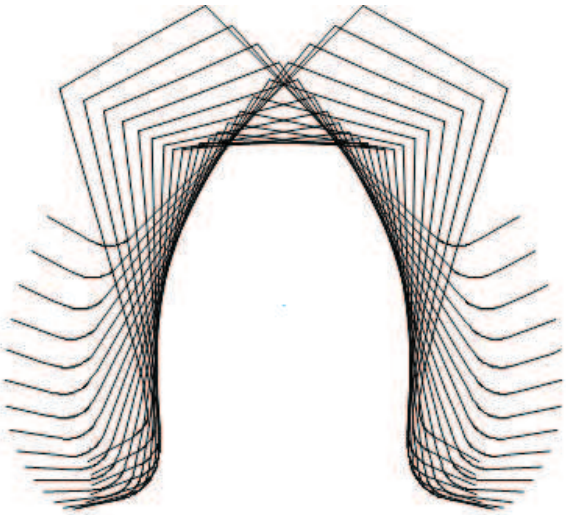

a) $\phi_u = \phi_l = 14.5^{\circ}$, $\eta_{fu} = \eta_{fl} = 0.209\, m_o$, $r_{tu} = r_{tl} = 0$ and $x_u = x_l = 0$

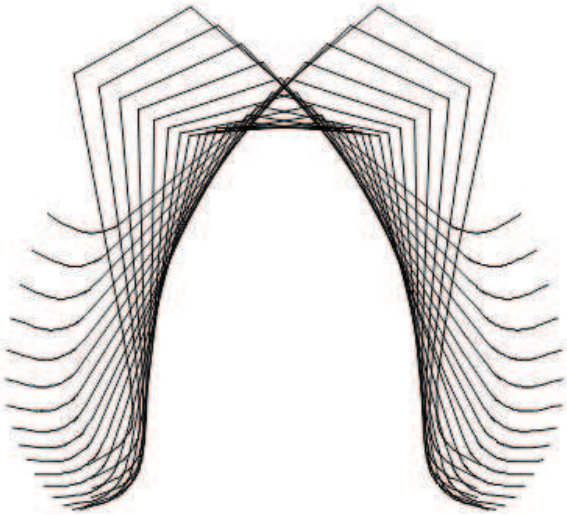

b) $\phi_u = \phi_l = 20^{\circ}$, $\eta_{fu} = \eta_{fl} = 0.3\, m_o$, $r_{tu} = r_{tl} = 0$ and $x_u = x_l = 0$

Figure 5. Samples of symmetric involute gear teeth shapes generation for $m_o = 10$ mm, $z = 14$ teeth, $h_a = m_o$ and $h_d = 1.157\, m_o$. These samples are magnified by scale (2.5:1).

 

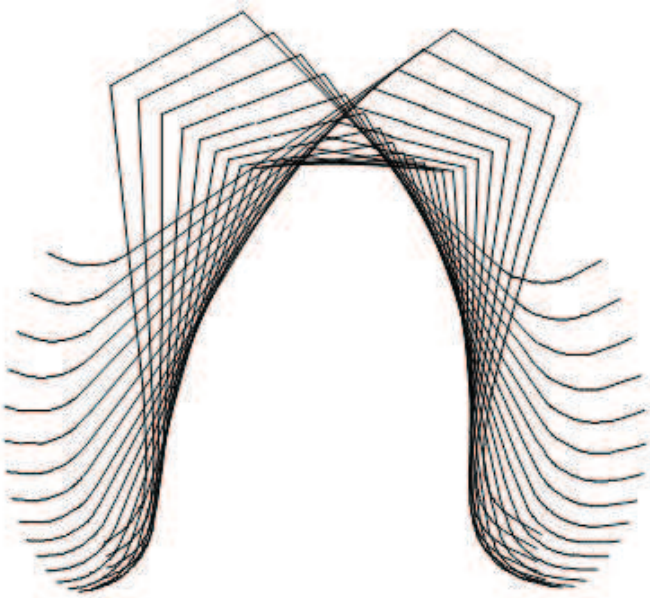

a) $\phi_u = 25^\circ$, $\phi_l = 14.5^\circ$, $r_{fu} = r_{fl} = 0.39\, m_o$, $r_{tu} = r_{tl} = 0$ and $x_u = x_l = 0$

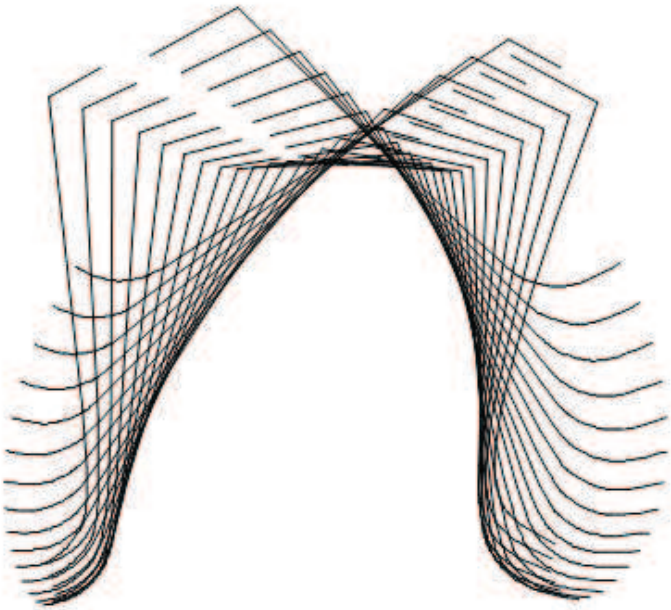

b) $\phi_u = 25^\circ$, $\phi_l = 14.5^\circ$, $r_{fu} = r_{fl} = 0.39\, m_o$, $r_{tu} = r_{tl} = 0$, $x_u = 0.5$ and $x_l = 0$

Figure 6. Samples of asymmetric involute gear teeth shapes generation for $m_o = 10$ mm, $z = 14$ teeth, $h_a = m_o$ and $h_d = 1.25\, m_o$. These samples are magnified by scale (2.5:1).